EXAFS studies of rare-earth metaphosphate glasses

D. T. Bowron,* G. A. Saunders,† R. J. Newport, B. D. Rainford,‡ and H. B. Senin§
Physics Laboratory, The University of Kent, Canterbury, CT2 7NR, United Kingdom
(Received 6 March 1995; revised manuscript received 5 October 1995)

An extended x-ray-absorption fine structure (EXAFS) study has been carried out on a range of rare-earth metaphosphate $R(PO_3)_3$ glasses of growing interest in optical communications and laser technologies. Phosphate glasses modified using the rare-earth oxides Pr_6O_{11}, Nd_2O_3, Eu_2O_3, Gd_2O_3, Tb_2O_3, and Ho_2O_3, have been investigated using their respective rare-earth L_{III} absorption edges. The data provide information on the local environment of the rare-earth ion within the phosphate glass matrix constructed from linked PO_4 tetrahedra. The rare-earth ions occupy sites with an average coordination number in the range, $6 \leqslant N \leqslant 8$, the surrounding atoms being oxygen. The first shell interatomic distance over the range of rare-earth ions establishes the rare-earth contraction of ionic radii with increasing atomic number in a series of glasses. There is also evidence for a rare-earth-phosphorus correlation between 2.7 and 3.6 Å, and a further rare-earth-oxygen correlation at approximately 4 Å. The EXAFS spectrum shows no evidence for R-R correlations within the short-range order, a result especially pertinent to the optical and magnetic properties of the glasses. The fractal dimensionality $4C_{11}/B$ of these glasses, obtained from the elastic stiffnesses determined from ultrasonic wave velocities, ranges between 2.3 and 2.8, indicating that their connectivity tends towards having a three-dimensional character.

I. INTRODUCTION

The rare-earth metaphosphate glasses $(R_2O_3)_{0.25}(P_2O_5)_{0.75}$ (where R represents one of the rare-earth elements Ce, Pr, Nd, Sm, Eu, Gd, Tb, Dy, Ho, and Er or La or Y) display a plethora of unusual physical properties of both fundamental interest and potential application in laser and optoelectronics technology. The rare-earth ions are incorporated into the glass matrix in large modifier concentrations rather than at the low dopant levels usually employed in optoelectronic devices (and in this sense the current systems bear comparison with rare-earth-doped fluorite glasses.[1] These ions provide the electronic energy level structure required for optical devices such as glass host lasers and optical amplifiers. Rare-earth metaphosphate glasses are unusually stable to water, making them particularly suitable for device applications. In the cases of glasses containing europium[2] or gadolinium[3] the metaphosphate $R(PO_3)_3$ is a particularly stable composition; this has now been shown to be true in other systems comprising phosphate glasses modified by very high concentrations of rare-earth ions. The development of a fundamental understanding of their interesting optical and vibrational properties has been hampered by a lack of knowledge of their structures on the atomic scale. Indirect structural information has been gleaned from the Raman spectra which have identified that the vibrational modes are consistent with the network skeleton being comprised of linked PO_4 tetrahedra.[2,4–6] A recent direct structural study[7] employing the complementary probes extended x-ray-absorption fine structure (EXAFS) and x-ray diffraction has verified that the terbium metaphosphate $(Tb_2O_3)_{0.26}(P_2O_5)_{0.74}$ glass does have a network built up from PO_4 tetrahedral units. To obtain information about the local environment of the rare-earth ion within the phosphate glass matrix, an EXAFS study, using their respective rare-earth L_{III} absorption edges, has now been carried out on a range of metaphosphate glasses modified with the rare-earth oxides Pr_6O_{11}, Nd_2O_3, Eu_2O_3, Gd_2O_3, and Ho_2O_3. The glasses have been characterized by measurements of their compositions, densities, elastic stiffnesses, and bulk moduli. EXAFS, being an atom-type specific probe, is an ideal method for obtaining direct information on the short-range structural environment of the rare-earth atoms. As a technique it has advantages over x-ray diffraction in that it provides pair distribution functions containing only atomic correlations involving the atom whose absorption spectra is being probed; x-ray diffraction leads to a composite radial distribution function in which all atom pairs in the material are represented, weighted by the square of their respective atomic numbers.

To assess the fractal dimensionality, which provides additional valuable structural information about the connectivity of the glass network, the elastic stiffnesses have been determined, using the ultrasonic pulse echo overlap technique, for the same glasses whose structures have been investigated by EXAFS.

II. EXPERIMENTAL PROCEDURE

Rare-earth metaphosphate glasses were prepared by methods described in Ref. 5. High-purity dry rare-earth oxide and P_2O_5 were mixed in preweighed proportions in alumina crucibles. This mixture was then heated in an electric furnace to approximately 1500 °C which produced a melt of the oxide components, this melt was then poured into preheated (500 °C) steel moulds and allowed to cool. The chemical compositions and the densities of the resulting glasses are given in Table I. The results of electron probe quantitative analysis showed that like other rare-earth phosphate glasses,[2,3] regardless of the starting constituent ratios the compositions of glasses turned out to be similar, or slightly lower and close to that expected $(R_2O_3)_{0.25}(P_2O_5)_{0.75}$ which

TABLE I. The elastic and nonlinear acoustic vibrational properties of rare-earth phosphate glasses.

Glass composition (mole fraction)		Density (kg/m^3)	Elastic moduli (GPa)			Fractal dimension	Hydrostatic pressure derivatives of elastic stiffness		
			C_{11}	C_{44}	B	$\left(\frac{4C_{44}}{B}\right)$	$\left(\frac{\partial C_{11}}{\partial P}\right)_{P=0}$	$\left(\frac{\partial C_{44}}{\partial P}\right)_{P=0}$	$\left(\frac{\partial B}{\partial P}\right)_{P=0}$
Pr:	0.216	3094	67.9	23.4	36.7	2.55	0.84	−0.37	1.33
	0.254	3315	72.6	24.2	40.3	2.40	2.93	−0.03	2.97
	0.256	3338	74.3	24.3	41.9	2.32	2.52	0.64	1.67
Nd:	0.194	3121	69.1	23.6	37.6	2.51	3.87	−1.39	5.72
	0.196	3233	70.5	24.8	37.4	2.65	2.60	−1.30	4.33
	0.235	3358	72.2	26.1	37.4	2.79	1.81	0.14	1.63
	0.254	3497	73.6	24.9	40.4	2.46	2.30	−0.05	2.36
Eu (Ref. 2):	0.186	3182	71.1	23.9	39.2	2.44	−2.94	−1.06	−1.53
	0.200	3204	69.9	23.5	38.6	2.44	−2.97	−1.39	−1.12
	0.208	3215	69.2	23.2	38.3	2.42	−3.21	−1.51	−1.20
	0.218	3260	69.0	23.1	38.2	2.42	−3.35	−1.56	−1.27
	0.252	3438	70.4	23.2	39.5	2.35	−2.05	−0.99	−0.73
Gd (Ref. 3):	0.222	3339	68.4	23.2	37.5	2.48	0.73	−0.37	1.22
	0.226	3362	68.0	23.1	37.2	2.48	−0.18	−0.54	0.53
	0.229	3371	66.6	23.0	36.0	2.56	−0.61	−0.57	0.15
	0.245	3415	68.3	23.5	37.0	2.54	−0.47	−0.60	0.33
	0.250	3535	71.6	25.0	38.2	2.62	0.21	−0.62	0.85
Tb:	0.226	3435	73.9	24.2	41.6	2.33	−1.57	−0.74	−0.58
	0.247	3501	74.8	25.4	40.9	2.48	−1.58	−0.68	−0.67
	0.263	3578	76.2	25.7	42.0	2.45	−0.54	−0.82	0.56
	0.271	3666	78.3	25.3	44.5	2.27	+0.60	−0.49	1.25
Ho:	0.208	3327	73.1	24.7	40.1	2.46	−0.82	−0.50	−0.15
	0.220	3347	72.2	24.1	40.1	2.40	−0.55	−0.24	−0.24
	0.231	3516	76.1	24.1	43.9	2.20	−0.36	−0.16	−0.14

corresponds to the metaphosphate composition.

For the purposes of the EXAFS experiments, small pieces of these glass samples were powdered, first by crushing between two steel plates, then in a mortar and pestle. Phosphate glasses are generally highly susceptible to water contamination, but in the case of rare-earth metaphosphate glasses they appear to be exceptionally water resistant. Nevertheless, as a precaution, the samples were kept in as dry an environment as possible, sealed in containers containing silica gel. For the actual experiment, the powdered glass sample was dusted between sticky tape which was then placed into the x-ray beam, several layers often being required to ensure uniformity across the beam area, and to obtain an acceptable absorption edge step. The EXAFS experiments were performed using line 7.1 at the SRS, Daresbury Laboratory, UK, which offers access to the entire energy range required for a study of the rare-earth L_{III} absorption edges (5–12 keV) via a silicon (111) double crystal order sorting monochromator. The edges probed as part of this study are shown in Table II.

TABLE II. Rare-earth L_{III} absorption edges.

Pr	5969 eV	Nd	6216 eV
Eu	6985 eV	Gd	7252 eV
Tb	7521 eV	Ho	8076 eV

The EXAFS spectra were taken in standard transmission mode, the data giving an analyzable **k** range from 2 $Å^{-1}$ to between 9 and 12 $Å^{-1}$ depending on the edge being studied (note that this corresponds to $4<\mathbf{k}<18/24$ $Å^{-1}$ in the more usual diffraction formalism). The energy range is limited due to the presence of the rare-earth L_{II} absorption edge. The shorter **k** range reduces the real-space resolution for the determination of interatomic distance information, a problem that is, unfortunately, intrinsic to the systems being studied.

III. ELASTIC STIFFNESS AND FRACTAL DIMENSIONALITY OF THE RARE-EARTH METAPHOSPHATE GLASSES

The elastic stiffness and bulk moduli of the glasses (Table I), determined from ultrasonic wave velocity measurements at room temperature and atmospheric pressure, have similar values to those obtained for other rare-earth metaphosphate glasses studied previously.[2,3,5,8,9] Correspondence between the bulk and stiffness tensor components would be expected, if the glasses were to have similar structures. The elastic stiffnesses depend upon the bonding in the glass and can be used to provide useful information about the connectivity of the network by reference to the fractal dimensionality. Bergman and Kantor,[10] considering a two-dimensional Sierpinski gasket as the fractal object in a study of the critical behavior

of a random, d-dimensional, isotropic, elastic medium, have shown that the effective fractal dimensionality d of an inhomogeneous random mixture of fluid and a solid backbone at threshold is given by $4C_{11}/B$. Bogue and Sladek[11] have used the fractal dimensionality d, which should vary from 3 for 3-d networks of tetrahedral coordination polyhedra to 2 for 2-d structures and to 1 for 1-d chains, to assess the network connectivity of glasses. A fractal dimensionality d of close to unity obtained for a pure $AgPO_3$ metaphosphate glass[11] is consistent with a skeletal structure comprised of weakly linked chains of interconnected middle PO_4 tetrahedra. By contrast, the fractal dimensionality of the rare-earth metaphosphate glasses $R(PO_3)_3$ is between 2.2 and 2.8 (Table I), which implies a marked degree of cross linkage, as would be anticipated for modifier cations whose valence is greater than unity, or increased branching of the network of PO_4 chains facilitated by an increase in the number of end and branching units incorporated into the basic phosphate network. This agrees with the coordination numbers found from the EXAFS study (Sec. IV).

IV. EXAFS STRUCTURAL DETERMINATIONS

A. Theory and analysis procedures

The EXAFS data analysis was performed using the standard Daresbury Laboratory EXAFS analysis suite of programs, namely EXCALIB, EXBACK, and EXCURV90,[12] which respectively perform the tasks of (i) summation of multiple data sets and calibration of their edges and absorptions, (ii) background subtration and normalization of the EXAFS signal, (iii) fitting of the EXAFS spectrum by means of the fast curved wave theory.[13,14]

Examination of the phenomenological plane-wave equation, which can be used to describe the EXAFS spectra, is useful to show the relationships between the various theoretical parameters:

$$\chi(k)=A(k)\sum_i \frac{N_i}{kR_i^2}|f(k,\pi)_i|\sin(2kR_i+2\delta+\varphi_i) \times \exp\left[\frac{-2R_i}{\lambda}\right]\exp[-2\sigma_i^2k^2].$$

In EXAFS, **k** is the wave vector of the freed photoelectron. Note the direct correlation in the two variables $A(k)$ and N_i. $A(k)$ typically varies between 0.6 and 0.8, dependent upon the atomic number of the excited atom type. It is one of the main parameters which needs calibration if dependable atomic coordination numbers are to be extracted from the data. In this work a crystalline neodymium ultraphosphate (NdP_5O_{14}) sample was used as the calibrant system, since it is a well-characterized material.[15] The other parameters in this expression are R_i, the distance between the excited atom and the neighboring electron backscattering atom i, $f(k,\pi)_i$ a measure of the strength of backscattering of the atom type i, δ_i is the phase shift induced in the electron wave as it propagates through the excited atom potential, whilst φ is the phase shift induced by the backscattering atom potential; λ is a mean free path term to account for the finite lifetime of the propagating electron wave and σ is the exponent in the Debye-Waller term to account for static and vibrational disorder in the structural system under examination

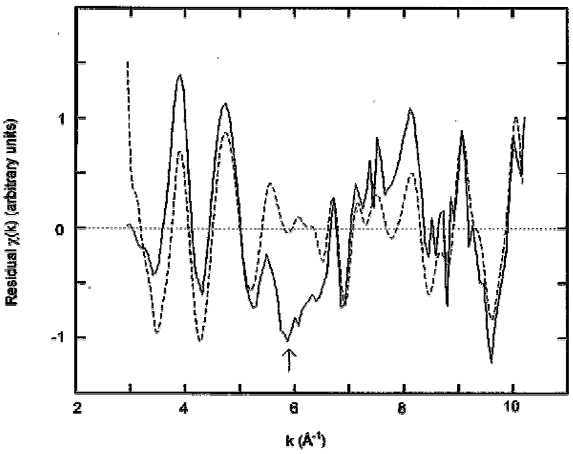

FIG. 1. Residual function after a first shell model fit is subtracted from the raw experimental metaphosphate glass data; before (solid line) and after (dashed line) Fourier filtering to remove the anomalous feature at ~6 $Å^{-1}$ (marked by the arrow) which is most likely an artifact of a double-electron excitation event.

The plane-wave equation is a useful heuristic model for EXAFS, but is not used in the EXCURV90 (Ref. 12) code; this uses the far more reliable fast curved wave theory[13,14] or the small atom approximation.[16]

When performing the background subtraction step of the initial data preparation stages of the analysis, it was noticed that there appears to be a step function evident in the rare-earth spectra between k=5 and 7 $Å^{-1}$ (Fig. 1), this is possibly evidence for the presence of a double-electron excitation[17] of the $4d_{5/2}$ electrons present in the rare earths. Such an excitation would be manifest at this position since it corresponds to electron binding energies in the range 109–196 eV (5.3–7.1 $Å^{-1}$), for cerium to lutetium, and would result in a discontinuity in the background x-ray-absorption function. If this discontinuity is not accounted for in the background substraction and normalization stage of data analysis, it results in a peak in the Fourier transform of the EXAFS spectra, occurring at an unphysically low interatomic distance; this effect is shown if Fig. 2, which is the atomic pair distribution function obtained from the EXAFS signal after removal of a first atomic shell model. The simplest method for removing this effect is to Fourier filter the experimental spectra, removing contributions at small distances, otherwise the correction can be made at the initial background subtraction stage by fitting a function with a discontinuity occurring at the double-electron excitation energy. Poor background subtraction can, in general terms, lead to difficulties when fitting model parameters to the experimental function; effects include poor determination of atomic species type from backscattering phase parameters due to signals being corrupted by low-frequency components that have not been removed. In the case of these glasses, the presence of the contaminant feature in the background function is adequately removed by a simple Fourier filtering process since this anomalous feature in the background signal resulted in a relatively well-defined pair distribution function (PDF) contaminant peak at low R. The effect of removal of

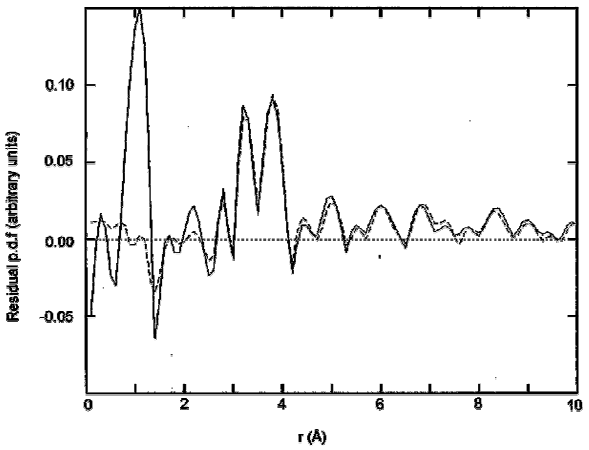

FIG. 2. Fourier transform of the residual functions shown in Fig. 1, demonstrating the unphysical low-r feature in the uncorrected Fourier transform (solid line) and its absence from the corrected residual's transform.

this peak can be seen in Fig. 1, the resulting corrected residual component after fitting the first atomic shell oscillates more evenly about the axis and allows the extraction of the correlations contained in the remaining signal, this process is not exact and consequently the errors in the higher shell correlations are greater.

B. Calibration of EXAFS data

To calibrate the constants necessary for determination of the structural information contained in the EXAFS spectra from the glass samples, data were collected from the crystalline neodymium ultraphosphate sample (NdP_5O_{14}) at a temperature of 105 K, the atomic structure of this material being known.[15] As for other rare-earth-oxide materials, the local structure of this compound is rather complex, consisting of eight oxygen atoms surrounding each neodymium atom at seven slightly different distances: 2.38, 2.40, 2.40, 2.41, 2.46, 2.47, 2.49, 2.50 Å.

Unfortunately EXAFS as an experimental technique does not have the resolution to individually isolate each of these distances, a particularly severe problem at the rare-earth L_{III} edges, due to the short accessible **k** range. Hence it proved necessary to use a more simplistic model of the local structure about the neodymium, this being a two-shell model of four oxygen atoms at 2.398 Å and a further four oxygen atoms at 2.48Å, these values being the mean values of the four short interatomic distances and four longer interatomic distances, respectively. The Debye-Waller factors associated with these shells were set to have typical crystalline values for σ^2 of 0.005 $Å^2$. Once this model had been set up, the nonstructural parameters in the EXAFS analysis were allowed to float in an iterative procedure, $A(k)$ notably refining to a value of 0.7, in close agreement with the value of 0.73 determined by Malet *et al.*[18] in their study of rare-earth oxides. In addition we note that the transferability of, and similarity between rare-earth phase shifts and analysis parameters has also been investigated by Catlow *et al.*[1]

Once the nonstructural parameters had been determined for the calibrant compound NdP_5O_{14} (which has a reasonably similar chemical environment to that thought to prevail in the metaphosphate glass samples), these parameters were then used as fixed information during the analysis of the series of rare-earth metaphosphate glasses. It has been found in other studies, e.g., Ref. 18, that the calibration of these parameters for rare-earth systems is reasonably transferable. In the worst case for the more distant rare-earth species from our chosen calibrant the errors which can arise in the coordination numbers due to miscalibration of the amplitude reduction factor would be of the order of $\pm 10\%$

C. Structural information obtained from EXAFS

The results obtained for the EXAFS spectra taken at the respective rare-earth L_{III} absorption edges, for the range of rare-earth metaphosphate glasses investigated, are summarized in Table III. All spectra were filtered to remove a low-frequency component peaking in the Fourier transform at approximately 1 Å.

Figures 3–6 show the theoretical and experimental fits and Fourier transforms obtained for each sample. The errors quoted in Table III are purely statistical, being calculated by the methods of Joyner *et al.*[19] The real error associated with the interatomic distances is estimated to be of the order of ± 0.05 Å and that of the coordination number to be at best ± 0.2 atoms if the calibrated value of the amplitude reduction factor is dependable.

The most striking trend evident in the data is the systematic contraction of the first shell rare-earth-oxygen distance from 2.38 Å for praseodymium metaphosphate glass to 2.20 Å in the holmium metaphosphate glass. This is consistent with the lanthanide contraction: the contraction in their ionic size as the period is traversed from lighter to heaver elements. No evidence for R-R correlations within the short-range order can be seen in the EXAFS spectrum, a finding which is likely to have important ramifications in the context of attempts to explain the optical and magnetic properties of these glasses containing very high concentrations of rare-earth ions. Models were tried which involved rare-earth-rare-earth correlations in the 3–4 Å range, but all failed to converge upon satisfactory solutions and beyond these distances the sensitivity of the EXAFS technique is not optimum.

The first shell coordination numbers generally fall between 6 and 8 for oxygens about a rare-earth ion. This coordination hints at a pseudo-octahedral or cubic arrangement of the oxygens or an admixture of these two configurations, rare-earth oxides characteristically having an octahedral arrangement for oxygens about rare-earth ions.

There is evidence in some samples for the second shell being a rare-earth-phosphorus correlation, but the errors are large, along with the distribution in coordination numbers and distances allocated. However the second rare-earth-oxygen correlation proved to be more consistent between samples with an associated distance of between 3.8 and 4.1 Å, although the variation in coordination number is still large, i.e., between 1 and 5 oxygens. This wide variation in results for parameters associated with more distant atomic shells is partly due to the amorphous nature of the material, i.e., the lack of any firm short-range order beyond the first interatomic correlation, and possibly through the increased

TABLE III. Structural parameters determined from the EXAFS spectra obtained for the rare-earth metaphosphate glasses.

Glass	Composition	Atomic shell correlation	Coordination number (atoms)	Distance (Å)	σ^2 (Å)
Praseodymium	$(Pr_6O_{11})_{0.216}$	Pr-O	7.1±0.2	2.38±0.002	0.013±0.0005
	$(P_2O_5)_{0.794}$	Pr-P	1.4±0.2	2.92±0.004	0.009±0.002
		Pr-O	4.0±0.4	4.08±0.004	0.006±0.001
Neodymium	$(Nd_2O_3)_{0.235}$	Nd-O	10.4±2.7	2.35±0.010	0.019±0.003
	$(P_2O_5)_{0.765}$	Nd-P	6.8±16.6	2.92±0.102	0.053±0.061
		Nd-O	2.0±0.7	3.82±0.005	0.005±0.004
Europium	$(Eu_2O_3)_{0.252}$	Eu-O	7.6±0.2	2.28±0.002	0.013±0.001
	$(P_2O_5)_{0.748}$	Eu-P	1.6±0.8	3.64±0.017	0.005±0.006
		Eu-O	1.0±0.6	4.00±0.015	0.001±0.005
Gadolinium	$(Gd_2O_3)_{0.25}$	Gd-O	5.7±0.3	2.27±0.002	0.007±0.001
	$(P_2O_5)_{0.75}$	Gd-P	1.3±0.3	2.71±0.005	0.008±0.002
		Gd-O	1.4±0.2	3.23±0.006	0.006±0.002
		Gd-O	2.1±0.3	3.94±0.005	0.002±0.001
Terbium	$(Tb_2O_3)_{0.26}$	Tb-O	8.0±0.2	2.25±0.002	0.014±0.0004
	$(P_2O_5)_{0.74}$	Tb-O	5.4±0.9	3.92±0.008	0.016±0.003
Holmium	$(Ho_2O_3)_{0.231}$	Ho-O	7.0±0.1	2.20±0.001	0.011±0.0002
	$(P_2O_5)_{0.769}$	Ho-O	5.5±0.6	3.89±0.004	0.013±0.002

uncertainty in the experimental signal components most likely from imperfect background function removal of the double-electron excitation features.

The values of σ presented in Table III correspond to a combined measure of the static and thermal disorder present in the system, i.e., a distribution in the evaluated interatomic distances (manifest in the Fourier transform of the EXAFS signal by the width of the peak, convoluted with a general experimental resolution function). It is likely that here, as for other glasses, the static disorder term will dominate, but a temperature study would be necessary if further information is to be obtained on the weightings of the particular contributions.

V. DISCUSSION

For phosphate glasses in general, chains, rings, and branched polymeric units of interconnected PO_4 tetrahedra can be produced by sharing oxygen atoms between the tetrahedra.[20] The recent study of a terbium metaphosphate glass[7] using the combination of x-ray diffraction and EXAFS techniques, establishes that rare-earth metaphosphate glass is built up from PO_4 tetrahedral units, most likely with pairs of PO_4 tetrahedra sharing only one corner. A usual feature of phosphates is that, if resonance is first neglected, then one of the four oxygen atoms in a tetrahedron is doubly bonded to the phosphorus and does not contribute to the interatomic

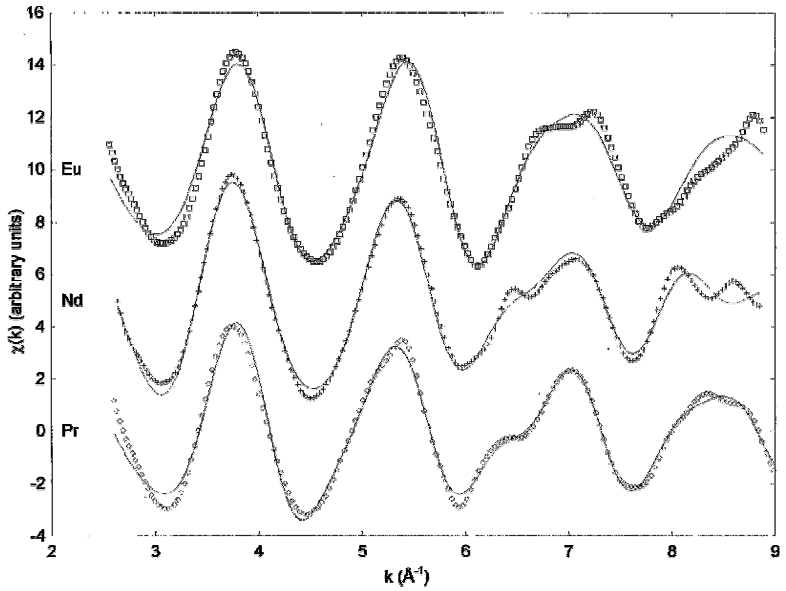

FIG. 3. Praseodymium, neodymium, and europium metaphosphate glass EXAFS χ (**k**), experimental data (points) and theoretical fits (lines).

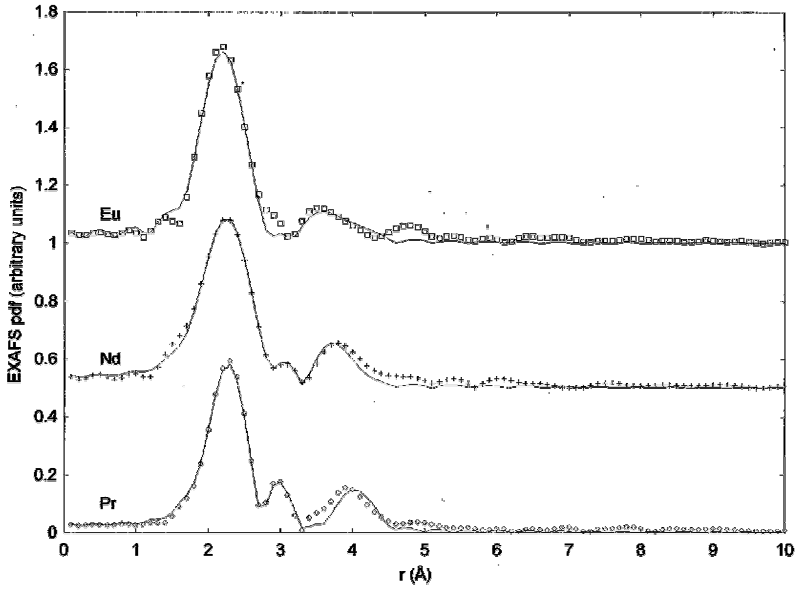

FIG. 4. Praseodymium, neodymium, and europium metaphosphate glass EXAFS PDF, experiment (points) and theory (lines).

bonding. In a phosphate tetrahedron the p-d orbital overlap responsible for the π bond is concentrated primarily between the P atom and its nonbridging oxygen ($P\text{-}O^-$). If the number of nonbridging oxygen atoms is reduced, then the average π character of the P-O bonds increases; an effect of such an increase would be to decrease the average P-O bond length.[21] The recent x-ray-diffraction study of terbium metaphosphate $(Tb_2O_3)_{0.26}(P_2O_5)_{0.74}$ glass showed that the first peak occurs at 1.58 ± 0.05 Å, characteristic of the P-O distance expected for linked PO_4 Q^2 tetrahedra (in the Q^n notation,[22] n being the number of nonbridging oxygens per tetrahedron). However that x-ray-diffraction experiment was unable to determine the P-O bond length to an accuracy sufficient to provide a measure of the exponent n in Q^n. EXAFS cannot resolve this interesting question. The way in which the PO_4 tetrahedra link to make up the glass skeleton is another matter. In P_2O_5 each P^{5+} is bonded to three bridging (POP) oxygen atoms with bond values of 1.0 valence units and one terminating oxygen with 2.0 valence units.[21–23] Hence the P_2O_5 glass structure is based on Q^3 tetrahedra. In general the phosphate glass skeleton can be constructed from three types of building units: (i) the branching tetrahedron in which three oxygen atoms are shared with neighboring PO_4 units, (ii) the middle tetrahedron in which two oxygen atoms are shared with neighboring PO_4, and there is one negative charge which is neutralized by a cation, (iii) the end unit which has one oxygen shared with another PO_4, and there are two negative charges. Metaphosphates of a trivalent ion modifier R^{3+} have the formula $R(PO_3)_3$. In principle any structure made of middle groups completely will fit the metaphosphate formula: a metaphosphate structure comprised of chains or rings, with the O/P ratio of 3.0, would be made up of Q^2 tetrahedra. Well-known examples include the amorphous alkali metal and silver metaphosphates whose fundamental skeletal structures are comprised of long chains of interconnected middle PO_4 tetrahedra;[24]

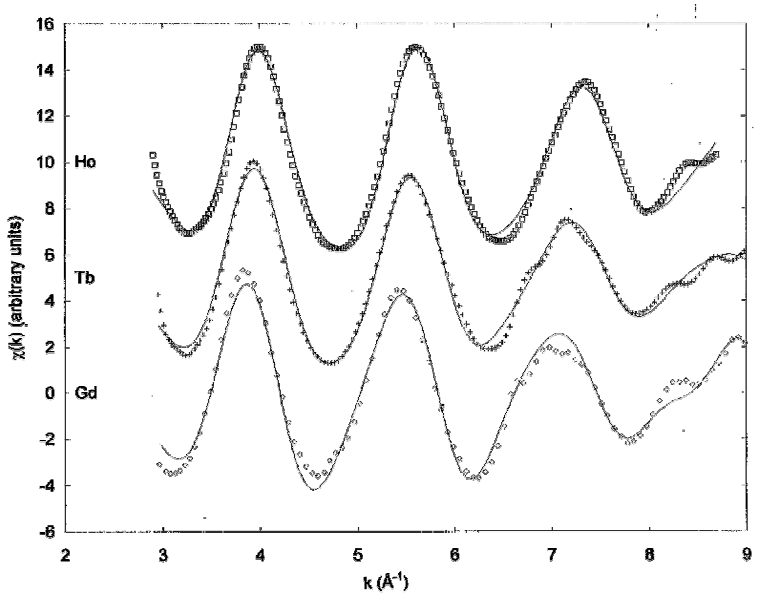

FIG. 5. Gadolinium, terbium, and holmium metaphosphate glass EXAFS $\chi(\mathbf{k})$, experimental data (points) and theoretical fits (lines).

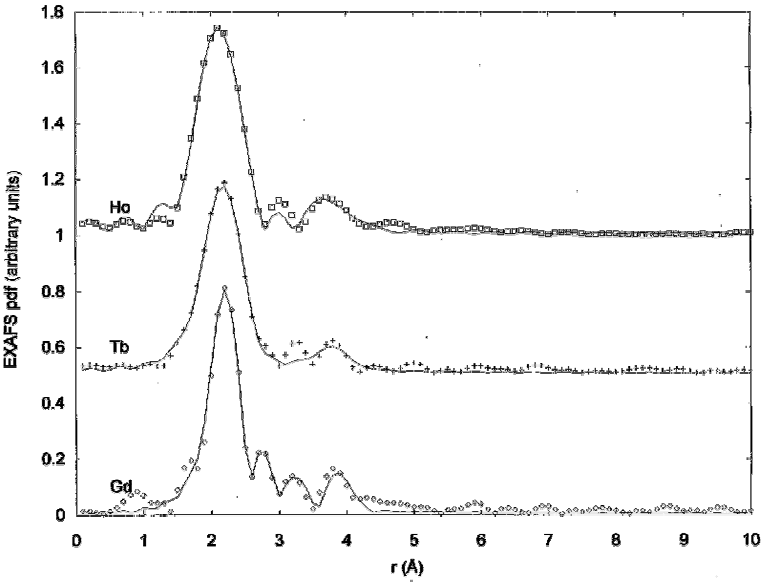

FIG. 6. Gadolinium, terbium, and holmium metaphosphate glass EXAFS PDF experiment (points) and theory (lines).

the fractal dimensionality of unity found for amorphous $AgPO_3$ (Ref. 11) is consistent with this. By contrast the fractal dimensionality of the rare-earth metaphosphate glasses $R(PO_3)_3$ lies between 2.2 and 2.8 (Table I): the structure of these glasses is close to having a three-dimensional character. There must be a strong degree of cross linkage, as might be expected for modifier cations whose valence is greater than unity. It seems that there is considerable branching in the PO_4 skeleton with consequent increase in the number of end and branching units. The coordination numbers (Table III) found for the rare-earth ions are consistent with this model: rare-earth ions would preferentially occupy interstices formed at branches in the network enabling them to bond ionically with this number of surrounding oxygens on PO_4 tetrahedra. These observations concerning the structure add weight to earlier assumptions of a model of a skeleton comprised of PO_4 tetrahedra linked via bridging oxygen atoms to interpret a wide range of vibrational and optical properties of the rare-earth metaphosphate glasses.[2–5,8,9,24] The high connectivity indicted by the fractal dimensionality of about 2.5 for each of the rare-earth metaphosphate glasses (Table I relates directly to the high coordination number of oxygen atoms surrounding each trivalent rare-earth ion and may also account for the unusually good resistance to moisture of these glasses, pinning by the rare-earth ions of the network and its nearly three-dimensional character reducing the susceptibility of the linked PO_4 groups to aqueous attack.

One property, among many, which is sensitive to the local symmetry about rare-earth ions is laser-induced fluorescence spectra. A rare-earth ion incorporated in glass or crystal matrix is subjected to a crystal field of the surrounding atoms and the Stark effect produces a group of levels for each single level of the free ion, the number of which can be determined using group-theoretical methods[25] and used to find, from fluorescence studies, information about the local symmetry.[26] In amorphous media, the emission observed from rare-earth ions consists of a superposition of contributions from individual ions distributed among the entire ensemble of local environments. The resulting statistical distribution of Stark components brings about a significant degree of inhomogeneous broadening of the absorption and emission lines. Recently fluorescence spectra measurements originating from SM^{3+} transitions in $(Sm_2O_3)_{0.248}(P_2O_5)_{0.752}$ glass have been shown[27] to be consistent with the rare-earth ion occupying the centre of a distorted cube comprised of four phosphate tetrahedrons. The coordination number of the rare-earth ion in such an arrangement is eight oxygens. This model is consistent with the EXAFS structural studies of the metaphosphate glasses (Table III).

VI. CONCLUSIONS

(1) The phosphate glass systems modified using the rare-earth oxides Pr_6O_{11}, Nd_2O_3, Eu_2O_3, Gd_2O_3, Tb_2O_3, and Ho_2O_3 show particularly stable metaphosphate compositions.

(2) The skeleton of these metaphosphate glasses is made up from linked PO_4 tetrahedra.

(3) The first shell coordination numbers fall between 6 and 8 for oxygens about a rare-earth ion suggesting an octahedral or cubic arrangement of the oxygens (or a mixture of both these configurations), consistent with those found in rare-earth oxides.

(4) An interesting feature is the observation of the lanthanide contraction in a series of glasses.

(5) Ultrasonic measurements of the elastic stiffnesses have been used to obtain fractal dimensionality $4C_{11}/B$; this ranges between 2.3 and 2.8, indicating that the connectivity of these glasses tends towards having a three-dimensional character.

ACKNOWLEDGMENTS

We are grateful to the Johnson Matthey Technology Centre (Dr. S. Bartlett) and to DRA Maritime Division (S. Takel) for support of our program of work on rare-earth phosphate glasses, and to the EPSRC for access to its synchroton x-ray facility. D.T.B. wishes to thank Pirelli General plc and the

University of Kent for financial support. H.B.S. is grateful to the University Pertanian Malaysia and the Government of Malaysia for financial support. We would also like to thank E. Schönherr of the Max-Planck-Institut für Festkörperforschung, Stuttgart, for preparing the crystalline NdP_5O_{14} used as an EXAFS calibrant, and Professor G.N. Greaves of the Daresbury Laboratory for providing us additional access to the SRS for the calibrant experiment.

*Current address: Department of Physics and Astronomy, University College London, Gower Street, London WC1E 6BT, UK.
†School of Physics, University of Bath, Claverton Down, Bath, BA2 7AY, UK.
‡Physics Department, University of Southampton, Highfield, Southampton, SO9 5NH, UK.
§Permanent address: Department of Physics, Universiti Pertanian Malaysia, 43400 Serdang, Selangor, Malaysia.

[1] C.R.A. Catlow, A.V. Chadwick, G.N. Greaves, and L.M. Moroney, Nature **312**, 601 (1984).
[2] H.M. Farok, H.B. Senin, G.A. Saunders, W. Poon, and H. Vass, J. Mater. Sci. **29**, 2847 (1994).
[3] H.B. Senin, G.A. Saunders, J. Li, and P.J. Ford, Phys. Chem. Glasses **35**, 109 (1994).
[4] K. Sun and W.M. Risen, Jr., Solid State Commun. **60**, 697 (1986).
[5] A. Mierzejewski, G.A. Saunders, H.A.A. Sidek, and B. Bridge, J. Non-Cryst. Solids **104**, 323 (1988).
[6] K.E. Lipinska-Kalita, A. Fontana, A. Leonardi, G. Carini, G. D'Angelo, G. Tripodo, and G.A. Saunders, Philos. Mag. **71**, 571 (1995).
[7] D. Bowron, R.J. Newport, B.D. Rainford, G.A. Saunders, and H.B. Senin, Phys. Rev. B **51**, 5739 (1995).
[8] H.A.A. Sidek, G.A. Saunders, R.N. Hampton, R.C.J. Draper, and B. Bridge, Philos. Mag. Lett. **57**, 53 (1988).
[9] H.A.A. Sidek, H.B. Senin, G.A. Saunders, and P.J. Ford, J. Fiz Mal. **14**, 11 (1993).
[10] D.J. Bergman and Y. Kantor, Phys. Rev. Lett. **53**, 511 (1984).
[11] R. Bogue and R.J. Sladek, Phys. Rev. B **42**, 5280 (1990).
[12] N. Binsted, J.W. Campbell, S.J. Gurman, and P.C. Stephenson, EXCURV90, Daresbury Laboratory, UK. EXAFS analysis program (1991).
[13] N. Binsted, S.J. Gurman, and I. Ross, J. Phys. C **17**, 143 (1984).
[14] N. Binsted, S.J. Gurman, and I. Ross, J. Phys. C **19**, 1845 (1986).
[15] H.Y-P. Hong, Acta Crystallogr. B **30**, 468 (1974).
[16] S.J. Gurman J. Phys. C **21**, 3699 (1988).
[17] J. Chaboy, J. García, A. Marcelli, and M.F. Ruiz-López, Chem. Phys. Lett. **174**, 389 (1990).
[18] P. Malet, M.J. Capitan, M.A. Centeno, J.A. Odriozola, and I. Carrizosa, J. Chem. Soc. Faraday Trans. **90**, 2783 (1994).
[19] R.W. Joyner, K.J. Martin, and P. Meehan, J. Phys. C **20**, 4005 (1987).
[20] S.W. Martin, Eur. J. Sol. Stat. Inorg. Chem. **28**, 271 (1991).
[21] R.K. Brow, R.J. Kirkpatrick, and G.L. Turner, J. Non-cryst. Solids **116**, 39 (1990).
[22] J.R. Wazer, *Phosphorus and its Compounds* (Interscience, New York, 1958), Vol. 1.
[23] R.K. Brow, J. Am. Ceram. Soc. **76**, 913 (1993).
[24] G. Carini, G. D'Angelo, M. Federico, G. Tripodo, G.A. Saunders, and H.B. Senin, Phys. Rev. B **50**, 2858 (1994).
[25] H. Bethe, Ann. Phys. **3**, 133 (1929).
[26] W.A. Runciman, Philos. Mag. **1**, 1075 (1956).
[27] H.M. Farok, G.A. Saunders, W. Poon, J. Crane, H. Vass, W. Hönle, and E. Schönherr (unpublished).